



# Simple hydrothermal synthesis and sintering of $\text{Na}_{0.5}\text{Bi}_{0.5}\text{TiO}_3$ nanowires

Xiangping Jiang, Mei Lin\*, Na Tu, Chao Chen, Shulan Zhou, Hongquan Zhan

Key Laboratory of Advanced Ceramic Materials, Department of Material Science and Engineering, Jingdezhen Ceramic Institute, Jingdezhen, 333001, Jiangxi, China

## ARTICLE INFO

### Article history:

Received 22 March 2011

Received in revised form 9 July 2011

Accepted 11 July 2011

Available online 23 July 2011

### Keywords:

Ceramics

Chemical synthesis

X-ray diffraction

Transmission electron microscopy

## ABSTRACT

Single-crystalline  $\text{Na}_{0.5}\text{Bi}_{0.5}\text{TiO}_3$  (NBT) nanowires, with diameters of 100 nm and lengths of about 4  $\mu\text{m}$ , were synthesized by using a simple hydrothermal method. Phase composition, morphology and microstructure of the as-prepared powders were characterized by X-ray diffraction (XRD), scanning electron microscopy (SEM) and transmission electron microscope (TEM). The effects of reaction temperature and reaction time on precipitation of the NBT nanowires were investigated. It was found that reaction time significantly influenced the growth behavior of the powders in the hydrothermal system. Based on the experimental results, the one-dimensional (1D) growth mechanism of the NBT was governed by a dissolution–recrystallization mechanism. NBT ceramics derived from the nanowires showed typical characteristics of relaxor ferroelectrics, with diffuseness exponent  $\gamma$  of as high as 1.73.

© 2011 Elsevier B.V. All rights reserved.

## 1. Introduction

1D nanostructure appears as an exciting research field for both its interesting physical properties and wide range of potential applications in nano-devices [1]. It is a product of oriented growth of materials, determined by its growth character and experimental conditions [2]. Templates, catalysts and other chemistry methods have been widely used to grow nanostructures, such as CuS [3],  $\text{TiO}_2$  [4], ZnO [5,6] and ZnS [7]. However, the introduction of templates or catalysts leads to a much more complicated process and may bring about an increase in impurity concentration in the final products [8]. New material systems and/or synthetic approaches are still being developed [9].

Bismuth sodium titanate,  $\text{Na}_{0.5}\text{Bi}_{0.5}\text{TiO}_3$  (NBT), which was found by Smolensky et al. [10], is considered to be an excellent candidate of lead-free piezoelectric ceramics. Its crystal structure is perovskite type with rhombohedral symmetry at room temperature. NBT possesses a relatively large remnant polarization ( $P_r = 38 \mu\text{C}/\text{cm}^2$ ) and high Curie temperature ( $T_c = 320^\circ\text{C}$ ). It is well known that NBT based ceramics have been actively studied for a long time because of their strong ferroelectric and piezoelectric properties [11–15].

Hydrothermal synthesis offers many advantages over conventional and nonconventional ceramic synthetic methods [16], such as energy saving, simplicity, cost effectiveness, better nucleation, higher dispersion, higher rate of reaction, better shape control, and lower temperature of operation in the presence of an appropriate

solvent and so on [17]. In recent years, many efforts have been made to prepare NBT nanostructures through hydrothermal method [18–22]. Liu et al. [19] obtained NBT monosized spherical particles in low concentrated NaOH solution (0.01–3 M) via a hydrothermal method. Liu et al. [20] synthesized NBT nanowhiskers via a sol–gel–hydrothermal method. However, sol–gel process is complex and hard to control. To date, the investigation for preparation of single-crystalline NBT nanowires is still lacking. In this work, a simple hydrothermal process was used to produce NBT nanowires at low processing temperature. Selected NBT nanowires were used to fabricate NBT ceramics. The objective of this study is to hopefully offer a promising technique to synthesize 1D nanostructure of other materials.

## 2. Experimental procedures

NBT nanocrystalline particles were synthesized via a hydrothermal method using reagent-grade sodium nitrate ( $\text{NaNO}_3$ ), bismuth nitrate pentahydrate ( $\text{Bi}(\text{NO}_3)_3 \cdot 5\text{H}_2\text{O}$ ), tetrabutyl titanate ( $\text{Ti}(\text{OC}_4\text{H}_9)_4$ ), acetic acid ( $\text{CH}_3\text{COOH}$ ) and ethanol ( $\text{CH}_3\text{CH}_2\text{OH}$ ) as the starting materials, and sodium hydroxide (NaOH) as mineralizer. On the whole, a bismuth concentration of 0.1 M and a stoichiometric Bi/Ti ratio of 0.5 were employed. Firstly,  $\text{Bi}(\text{NO}_3)_3 \cdot 5\text{H}_2\text{O}$  and  $\text{Ti}(\text{OC}_4\text{H}_9)_4$  were dissolved in  $\text{CH}_3\text{COOH}$  and  $\text{CH}_3\text{CH}_2\text{OH}$ , respectively.  $\text{NaNO}_3$  was dissolved in distilled water. Subsequently, the  $\text{NaNO}_3$ ,  $\text{Bi}(\text{NO}_3)_3 \cdot 5\text{H}_2\text{O}$  and  $\text{Ti}(\text{OC}_4\text{H}_9)_4$  solutions were mixed together, then NaOH solution was added into the mixed solution to form a suspension under continuously stirring for 0.5 h. The initial concentrations of NaOH solution were 4, 6, 8, 10, or 12 M. Finally, the as-prepared mixture was sealed in a stainless steel autoclave with a filling capacity of 60%. Reactions were carried out at an appropriate temperature under auto-generated pressure for 48 h. The autoclave was then cooled down to room temperature naturally. The products were washed several times with distilled water until pH of the solution was 7 and then dried at  $80^\circ\text{C}$  in an oven.

The obtained powders were ground and mixed with 0.5 wt% polyvinyl alcohol (PVA) binder. The granulated powders were pressed into disks with a diameter of 12 mm under uniaxial stress of 12 MPa. Conventional sintering was performed at

\* Corresponding author. Tel.: +86 798 13979829710.  
E-mail address: [linmei0238@163.com](mailto:linmei0238@163.com) (M. Lin).

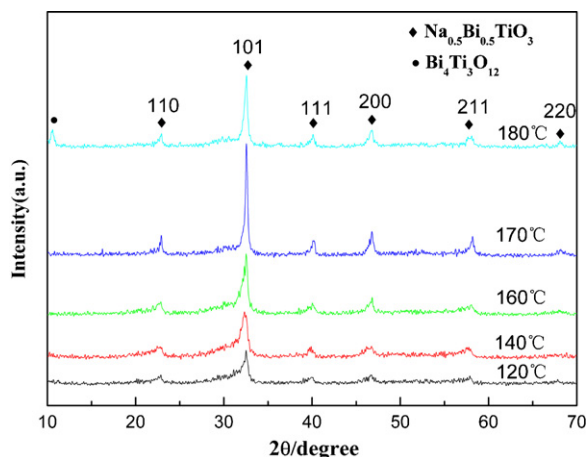


**Fig. 1.** XRD patterns of the NBT powders hydrothermally treated in 12 M NaOH for 48 h at different temperatures.

1170 °C for 2 h at a heating rate of 3 °C/min and cooling naturally. For dielectric measurements, silver paste was coated on both sides of the sintered specimens and fired at 800 °C for 30 min to form electrodes.

X-ray diffractions of the powders were performed on a Rigaku X-ray diffractometer with high-intensity Cu K $\alpha$  radiation. Crystalline and morphology of the NBT nanowires were characterized by using a JSM-6700F scanning electron microscopy (SEM), a JEOL-JEM 2010F transmission electron microscope (TEM) and selected area electron diffraction (SAED). Raman scattering measurements were carried out by using a HORIBA JOBIN YVON HR800 Raman spectrometer at room temperature. Dielectric measurements were carried out from room temperature to 500 °C at selected frequencies by using an Agilent 4294A precision impedance analyzer.

### 3. Results and discussion

**Fig. 1** shows XRD patterns of the powders hydrothermally treated under a NaOH concentration of 12 M for 48 h at different temperatures. Pure phase NBT powders were obtained at temperatures of 120–170 °C. With increasing reaction temperature, height of the diffraction peaks increased while the full-width at half-maximum decreased. NBT appeared at 120 °C and there was no impurity phase. However, the peak intensity was relatively low, which indicated the poor crystalline of the NBT powders. When the temperature was increased to 170 °C, well crystallized NBT powders were obtained. In addition, the sharpening of the diffraction peaks implies that the crystal growth was enhanced with the rise of reaction temperatures. However, as the temperature was further increased to 180 °C, impurity phase Bi<sub>4</sub>Ti<sub>3</sub>O<sub>12</sub> was detected, and the peaks of NBT were decreased. These results clearly showed that well crystalline phases of NBT were synthesized at 170 °C. **Fig. 2** shows SEM images of the NBT powders synthesized at 140 °C and 160 °C for 48 h NaOH of concentration of 12 M. At 140 °C, only spherical particles of about 1  $\mu$ m were observed (**Fig. 2(a)**). How-

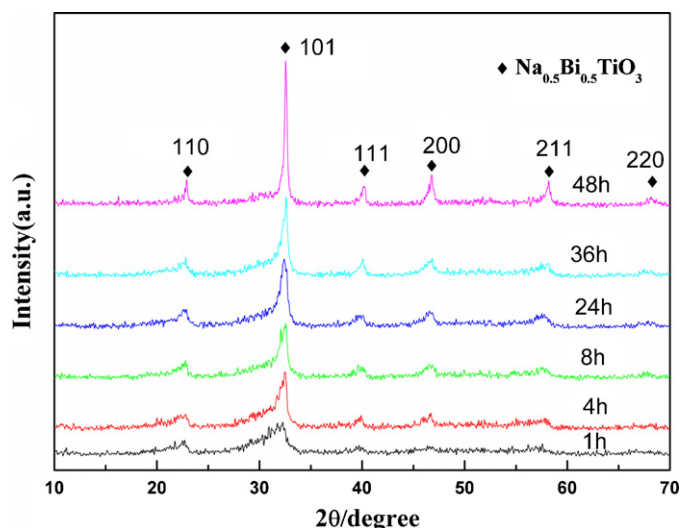


**Fig. 3.** XRD patterns of the NBT powders synthesized at 170 °C for various reaction times from 1 to 48 h.

ever, at 160 °C, a large amount of nanowires has been formed (**Fig. 2 (b)**).

The influences of reaction time were also investigated from 1 to 48 h at 170 °C in 12 M NaOH. **Fig. 3** shows XRD patterns of the samples with different reaction times. NBT could be detected after reacting for 1 h, but the peak intensity was low. It indicates that the crystalline of this sample was poor. The diffraction peaks became sharper and stronger as the reaction time was extended from 1 to 48 h, which suggests that a longer reaction time favors crystallization of the NBT powders. **Fig. 4** provides a set of SEM images of the samples prepared for different reaction times. As visualized in **Fig. 4(a)**, only spherical particles with a diameter of about 300 nm were obtained when the reaction time was 24 h. Interestingly, the morphology changed drastically when the reaction time was further extended. In addition to spherical particles, nanowires were also observed in the sample reacted for 36 h (**Fig. 4 (b)**). Meanwhile, they were agglomerated into big spherical particles with diameters of 1–2  $\mu$ m. On the other hand, the NBT nanowires were also agglomerated together. However, as illustrated in **Fig. 4(c)**, a large number of nanowires and a fibrous nanostructure of NBT were formed, accompanied by the disappearance of the spherical particles. These results indicated that reaction time played an important role in determining final morphologies of the NBT. Namely, morphology of the NBT powders can be controlled through varying the reaction time.

A typical TEM micrograph of the NBT powders synthesized at 170 °C for 48 h in 12 M NaOH solution is shown in **Fig. 5(a)**. It shows that the as-prepared products consisted of a large amount of nanowires. **Fig. 5(b)** shows a representative TEM image of a NBT

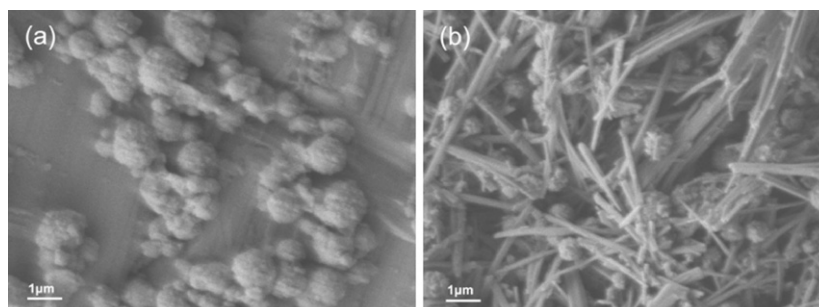


**Fig. 2.** SEM images of the NBT powders synthesized at reaction temperatures of 140 °C (a) and 160 °C (b) for 48 h in 12 M NaOH solution.

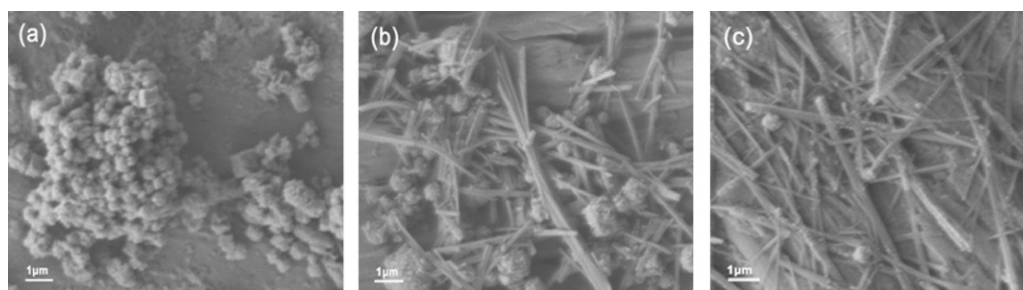


Fig. 4. SEM images of the NBT powders prepared at 170 °C for 24 h (a), 36 h (b) and 48 h (c).

nanowire. The width and length of the nanowire is nearly 100 nm and 4 μm, respectively, and the ratio (i.e., length/diameter) is about 40. Surface of the straight nanowire is smooth. The SAED pattern (Fig. 5(c)) obtained along a typical individual nanowire indicates that the nanowire is single crystal. The sharp diffraction spots can be indexed to the (2 2 0), (1 0 1) and ( $\bar{1}$  2 3) planes, which confirms the formation of crystalline rhombohedral NBT. The HRTEM image given in Fig. 5(d) further supports the single-crystalline nature of the NBT nanowires. The adjacent lattice spacing estimated from this image is 1.126 nm, which is corresponding to triple distance of the (1 1 0) crystal planes of 0.388 nm.

Room-temperature Raman spectrum of the NBT powders synthesized at 170 °C for 48 h in 12 M NaOH is shown in Fig. 6. The Raman bands for NBT are relatively broad, which is typical for relaxor-based perovskite ferroelectrics [23]. The broadening is mainly due to the cation disorder at the 12-fold coordinated site [24]. As can be seen, there are five obvious peaks appearing at about 118, 152, 284, 545 and 800  $\text{cm}^{-1}$  over 100–1000  $\text{cm}^{-1}$ , which is in

good agreement with the reported data [25,26]. For NBT, the low-frequency band at 118 and 152  $\text{cm}^{-1}$  is associated with the Na–O bonds, whereas the high-frequency bands of 284, 545 and 800  $\text{cm}^{-1}$  can probably be assigned to vibrations of the  $\text{TiO}_6$  octahedral. However, a Bi–O bond would be located at very low frequencies and was not observed here due to the high mass of bismuth atom.

There are two formation mechanisms proposed for the hydrothermal reactions: in situ transformation and dissolution–recrystallization. In this experiment, the formation of the nanowires can be attributed to dissolution–recrystallization mechanism, in which aqueous metal species were formed by dissolution of the precursors followed by recrystallization from the supersaturated solution [18]. The dissolving rate of  $\text{TiO}_2 \cdot n\text{H}_2\text{O}$  was much lower than that of  $\text{Bi}_2\text{O}_3 \cdot n\text{H}_2\text{O}$  [22], which resulted in a sluggish dissolution–crystallization process. Fig. 7 schematically outlines the major steps involved in the hydrothermal synthesis. During the early stage, the dissolved bismuth ions were supposed to be absorbed on surface of the  $\text{TiO}_2 \cdot n\text{H}_2\text{O}$  particles and then

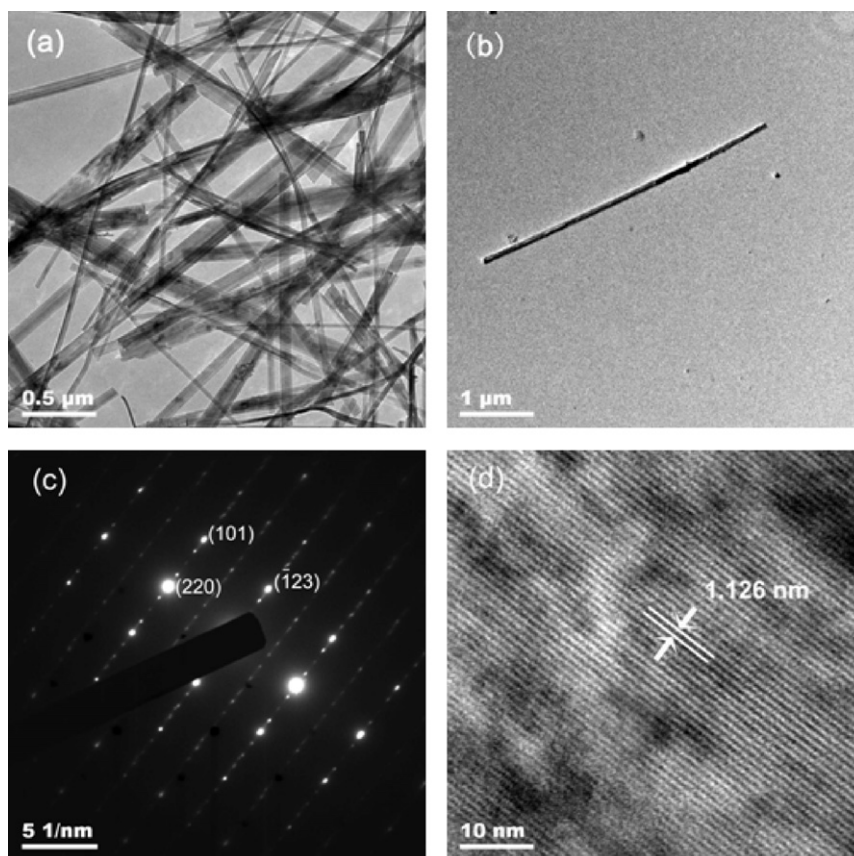


Fig. 5. (a) TEM photograph of NBT nanowires synthesized at 170 °C for 48 h in 12 M NaOH solution. (b) TEM image of a typical NBT nanowire. (c) SAED pattern of nanowires. (d) The HRTEM image of a nanowire with the interplanar spacing about 1.126 nm.

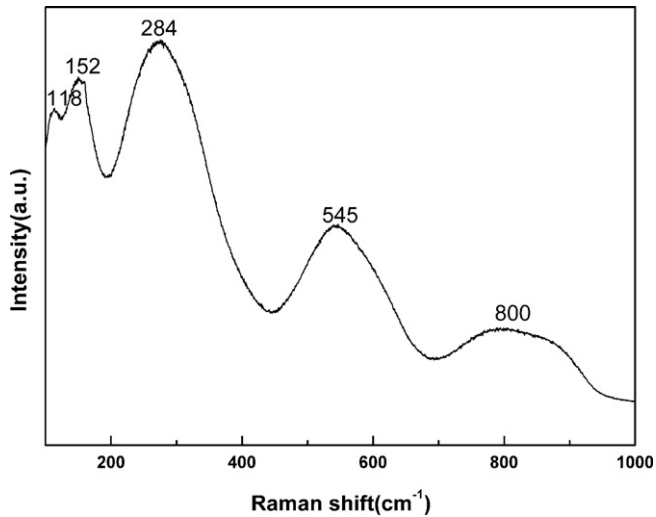


Fig. 6. Raman spectra of the NBT powders synthesized at 170 °C for 48 h in 12 M NaOH solution.

transferred into more stable NBT via in situ transformation process. Consequently, aggregated spherical particles were obtained. When the reaction time was extended to 36 h, more  $\text{TiO}_2 \cdot n\text{H}_2\text{O}$  particles were dissolved. This process might include rupture of the structure and dissolution of the spherical particles as well as the formation of the nanowires. After reacting for 48 h, it is believed that all  $\text{Na}^+$ ,  $\text{Bi}^{3+}$  and  $\text{Ti}^{4+}$  ions were homogeneously distributed in the solution

and crystalline perovskite nanowires were directly precipitated from the homogeneous solution via chemical reaction [18,27]. It can be concluded that a longer reaction time favors the formation of NBT nanowires. Thus, we believe that an ample reaction time is contributed to diffusion and transference of ions, which resulted in ions accumulated along the (001) direction and finally formed NBT nanowires.

Due to the good sinterability of the nano-size powders and pure NBT phase, the nanowires synthesized at 170 °C for 48 h in 12 M NaOH solution were selected to prepare ceramics. Fig. 8(a) shows SEM image of NBT ceramics derived from nanowires at 1170 °C for 2 h. As present, a homogenous and compact microstructure was obtained. Fig. 8(b) shows temperature dependence of relative permittivity  $\epsilon_r$  and dielectric loss  $\tan \delta$ . Obviously, the sample exhibits typical relaxor ferroelectric characteristics. The maximum in  $\epsilon_r$  is diffusive and centered at 340 °C. It also shows a feature of diffuse phase transition with a slight frequency dispersion occurring around Curie temperature. It can be seen that  $\epsilon_r$  and  $T_m$  exhibit strong dependency on frequency. Meanwhile,  $T_m$  gradually shifted toward lower temperature with increasing frequency. The specimen shows  $\epsilon_r$  of 2570 and  $\tan \delta$  of 0.055 at room temperature at 10 kHz.

To explain the dielectric behavior of complex ferroelectrics with diffuse phase transition, further studies were carried out by fitting the result of temperature dependency of dielectric permittivity to the modified Curie–Weiss law [28,29].

$$\frac{1}{\epsilon_r} = \frac{1}{\epsilon_m} + (C)^{-1}(T - T_m)^\gamma \quad (1)$$

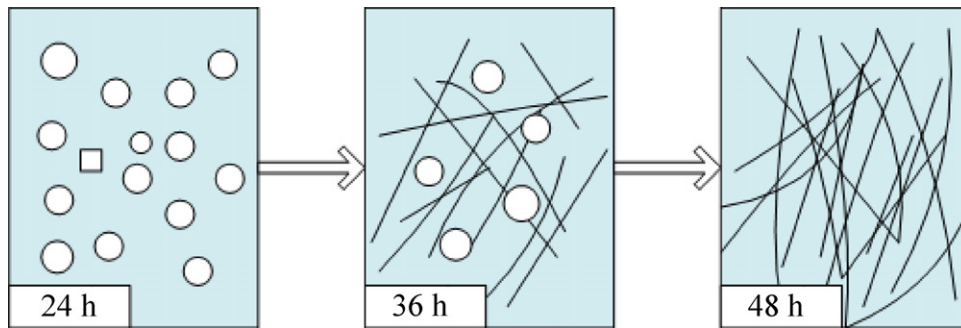


Fig. 7. A schematic illustration of major steps involved in the synthesis.

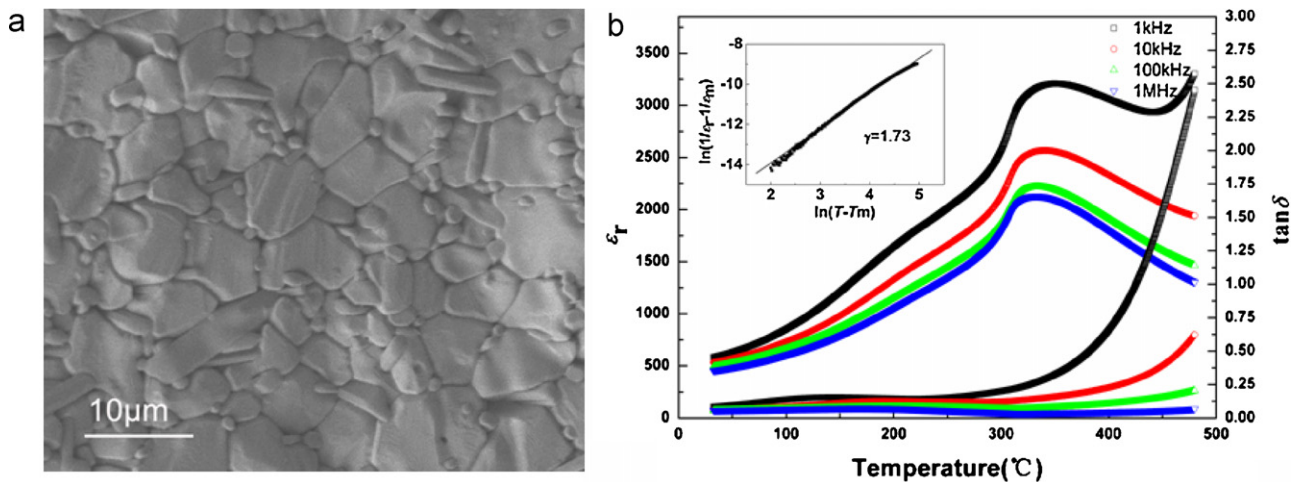


Fig. 8. (a) SEM image of the NBT ceramics sintered at 1170 °C for 2 h and (b) temperature dependence of relative permittivity  $\epsilon_r$ , dielectric loss  $\tan \delta$  at various frequencies for the NBT ceramics. Inset is  $\ln[(\epsilon_m/\epsilon)^{-1}]$  as a function of  $\ln(T - T_m)$  at frequencies of 10 kHz.

where  $\varepsilon_m$  is the maximum value of dielectric constant at the transition temperature ( $T_m$ ),  $C$  is the Curie-like constant.  $\gamma$  ( $1 < \gamma < 2$ ) is a constant, expressing the diffuseness exponent of the phase transition.  $\Delta$  is peak broadening parameter that indicates the diffuseness degree. Fig. 8(b) inset picture shows the plot of  $\ln[(\varepsilon_m/\varepsilon)^{-1}]$  as a function of  $\ln(T - T_m)$  at 10 kHz. A linear relationship was obtained by linear fitting to the experimental data. The slope of the fitting curve  $\gamma$  was 1.73, which is very close to 2 and indicates that the NBT ceramics have a large relaxor features. The relaxor behavior of the NBT ceramics can be attributed to the positional disorder between  $\text{Na}^+$  and  $\text{Bi}^{3+}$  cations on A site [30].

#### 4. Conclusions

High-purity NBT nanowires were synthesized by a simple hydrothermal method with no participation of catalysts or templates and requiring no expensive equipment. The results suggested that morphology of the powders was significantly influenced by reaction time. Single-crystalline nanowires of NBT with diameters of 100 nm and lengths of about 4  $\mu\text{m}$  were formed at 170 °C for 48 h in 12 M NaOH solution. The as-prepared NBT nanowires were highly crystalline and free from defects. The 1D growth mechanism of the NBT was dissolution–recrystallization. The NBT ceramics exhibited relaxor features. It is expected that this process could be a promising technique to synthesize 1D nanostructure of other materials.

#### Acknowledgements

We gratefully acknowledge financial support from National Natural Science Foundation of China (No: 50862005, 51062005, 91022027); Natural Science Foundation of Jiangxi (No: 2010GQW0037, 2010GQW0038); Foundation of Training Academic and Technical Leaders for Main Majors of Jiangxi (2010DD00800); Colleges and Universities “advanced ceramics” scientific and technological innovation team of Jiangxi; Foundation of Jiangxi Provincial Department of Education (No: GJJ10027, GJJ11196, GJJ11197, GJJ10226).

#### References

- [1] H. Kind, H.Q. Yan, B. Messer, M. Law, P.D. Yang, *Adv. Mater.* 14 (2002) 158.
- [2] J. Wang, Q. Chen, C. Zeng, B. Hou, *Adv. Mater.-Including Chem. Vapor Depos.* 16 (2004) 137.
- [3] X.L. Liu, Y.J. Zhu, *Mater. Lett.* 65 (2011) 1089.
- [4] K.L. Lv, J.G. Yu, L.Z. Cui, S.L. Chen, M. Li, *J. Alloys Compd.* 509 (2011) 4557.
- [5] A.K. Srivastava, M. Deepa, K.N. Sood, E. Erdem, R.A. Eichel, *Adv. Mater. Lett.* 2 (2011) 142.
- [6] M. Rajabi, R.S. Dariani, A. Iraj Zad, *J. Alloys Compd.* 509 (2011) 4295.
- [7] M. Lei, X.L. Fu, P.G. Li, W.H. Tang, *J. Alloys Compd.* 509 (2011) 5769.
- [8] X. Wang, Y. Li, *J. Am. Chem. Soc.* 124 (2002) 2880.
- [9] B. Gates, B. Mayers, A. Grossman, Y. Xia, *Mater. Sci.* 5 (2001) 143.
- [10] G.A. Smolensky, V.A. Isupov, A.I. Agranovskaya, *Sov. Phys. Solid State* 2 (1961) 2584.
- [11] Q. Xu, D.P. Huang, M. Chen, W. Chen, H.X. Liu, B.H. Kim, *J. Alloys Compd.* 471 (2009) 310.
- [12] W. Jo, J.E. Daniels, J.L. Jones, X.L. Tan, P.A. Thomas, D. Damjanovic, J. Rödel, *J. Appl. Phys.* 109 (2011) 014110.
- [13] Z.H. Chen, J.N. Ding, L. Mei, N.Y. Yuan, Y.Y. Zhu, *J. Alloys Compd.* 509 (2011) 482.
- [14] C.H. Wang, *Adv. Mater. Res.* 239 (2011) 3240.
- [15] K.A. Razak, C.J. Yip, S. Sreekantan, *J. Alloys Compd.* 509 (2011) 2936.
- [16] W.L. Suchanek, M.M. Lencka, R.E. Riman, in: D.A. Palmer, R. Fernández-Prini, A.H. Harvey (Eds.), *Aqueous Systems at Elevated Temperatures and Pressures: Physical Chemistry in Water, Steam, and Hydrothermal Solutions*, E-Publishing, Inc., Elsevier, 2004, 717 pp.
- [17] M. Yoshimura, K. Byrappa, *J. Mater. Sci.* 43 (2008) 2085.
- [18] X.Z. Jing, Y.X. Li, Q.R. Yin, *Mater. Sci. Eng. B* 99 (2003) 506.
- [19] Y.F. Liu, Y.N. Lu, S.H. Dai, *J. Alloys Compd.* 484 (2009) 801.
- [20] J.B. Liu, H. Wang, Y.D. Hou, M.K. Zhu, H. Yan, M. Yoshimura, *Nanotechnology* 15 (2004) 777.
- [21] Y.G. Wang, G. Xu, X.P. Ji, Z.H. Ren, W.J. Weng, P.Y. Du, G. Shen, G.R. Han, *J. Alloys Compd.* 475 (2009) L25.
- [22] T.L. Lu, J.H. Dai, J.T. Tian, W.W. Song, X.Z. Liu, L. Lai, H.J. Chu, X. Huang, X.Y. Liu, *J. Alloys Compd.* 490 (2010) 232.
- [23] M.R. Shen, G.G. Siu, Z.K. Xu, W.W. Cao, *Appl. Phys. Lett.* 86 (2005) 252903.
- [24] Y.D. Hou, M.K. Zhu, L. Hou, J.B. Liu, J.L. Tang, H. Wang, H. Yan, *J. Cryst. Growth* 273 (2005) 500.
- [25] J. Kreisel, A.M. Glazer, G. Jones, P.A. Thomas, L. Abello, G. Lucazeau, *J. Phys.: Condens. Matter* 12 (2000) 3267.
- [26] G.O. Jones, J. Kreisel, V. Jennings, M.A. Geday, P.A. Thomas, A.M. Glazer, *Ferroelectrics* 270 (2002) 191.
- [27] J. Moon, J.A. Kerchner, H. Krarup, J.H. Adair, *J. Mater. Res.* 14 (1999) 425.
- [28] K. Uchino, S. Nomura, *Ferroelectrics Lett. Sect.* 44 (1982) 55.
- [29] X.P. Jiang, L.Z. Li, M. Zeng, H.L.W. Chan, *Mater. Lett.* 60 (2006) 1786.
- [30] J.F. Yang, Y.D. Hou, C. Wang, M.K. Zhu, H. Yan, *Appl. Phys. Lett.* 91 (2007) 023118.